Plenary Paper Presented at 15th Annual Meeting of the *International Polymer Processing Society*, June 1999

Extensional rheometry of polymeric fluids and the uniaxial elongation of viscoelastic filaments

G. H. McKinley, S. L. Anna, A. Tripathi & Minwu Yao[2]
Department of Mechanical Engineering, M.I.T., Cambridge MA 02139, USA
[2]Ohio Aerospace Institute, Brookpark, OH 44132, USA

1. Introduction

For viscoelastic fluids such as polymer melts and solutions, the transient uniaxial extensional viscosity is a function of both the rate of stretching and the total deformation or strain imposed. Knowledge of the resulting material function is of great importance in governing the dynamics and stability of polymer processing operations such as fiber-spinning, film-blowing and blow molding. Filament stretching rheometers provide one of the few ways of unambiguously measuring the transient elongational response of 'mobile' polymeric fluids that are viscous ($1 \leq \eta \leq 1000$ Pa.s) but not rigid enough to test in the extensiometers commonly employed for extremely viscous melts such as polyethylene and polypropylene (Hosstetler & Meissner, 1994). However, even in these filament stretching devices the deformable nature of the free-surface of the test fluid and the no-slip boundary conditions pinning the liquid bridge to the endplates preclude truly homogeneous kinematics and it is essential to combine experimental measurements with computational rheometry in order to understand the dynamical characteristics of the device.

In the present work, we combine experimental measurements on polymer solutions and polymer melts in a temperature-controlled Filament Stretching Rheometer (FISER) with time-dependent finite-element numerical simulations using single and multi-mode formulations of the Giesekus model. During the imposed uniaxial elongation, numerical calculations are able to quantitatively simulate the measured stress growth in the materials. However, experiments and calculations show that the dynamical response of the fluid filament is strongly dependent on the exact form of the transient extensional viscosity. We show that even if a non-Newtonian fluid exhibits some strain-hardening, this can be insufficient to stabilize the contraction in the filament radius as the sample is exponentially elongated. Effects such as elastic recoil in parts of the filament result in a localized rate of thinning or 'necking' that is enhanced beyond that of a strain-independent Newtonian filament, and the elongating fluid thread can 'neck down' and break in a finite time. This qualitative difference compared with strongly strain-hardening elastic fluids can be understood in terms of a modified Considère analysis commonly employed for describing necking in tensile tests of solid polymer samples. Finally, following cessation of stretching at a finite strain, the tensile stresses in the elongated column rapidly relax and experiments and simulations show

that viscoelastic filaments undergo capillary-driven break-up at a rate that is greatly enhanced due to the fluid viscoelasticity. The dynamics of this filament failure are manifested in industrial processing operations through heuristic concepts such as '*spinnability*' and '*tackiness*' and are intimately connected to the transient uniaxial elongational stress growth of the polymeric material. Filament stretching devices are also natural platforms to probe such effects since they can monitor both the radial profile of the thinning filament and the resulting tensile force; they thus offer the possibility of extending our understanding of instability mechanisms such as necking and peeling of viscoelastic materials.

2. Operational Characteristics of Filament Stretching Devices

The basic operation of a filament stretching device is shown in Figure 1. Several variants of the basic configuration have been published (Tirtaatmadja & Sridhar, 1993; Spiegelberg *et al.* 1996; van Nieuwkoop *et al.* 1996). A small cylindrical plug of fluid (a *liquid bridge*) is generated between two flat disks of radius R_0 and stabilized against gravitational sagging by capillarity. The initial aspect ratio is denoted $\Lambda_0 = L_0/R_0$.

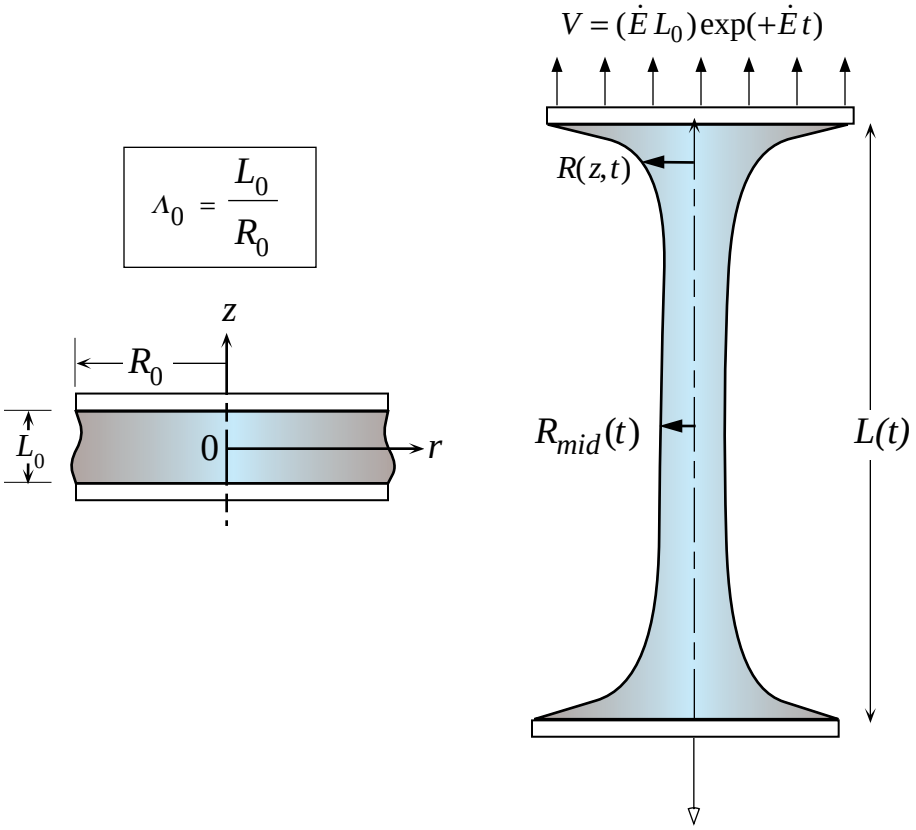

Figure 1 Schematic diagram of a filament stretching extensional rheometer (FiSER).

At time t = 0, the upper plate is set in motion and the resulting midpoint radius of the filament $R_{mid}(t)$ and tensile force $F_z(t)$ exerted by the elongating column are measured. The endplate velocity

profile $\dot{L}_p(t)$ is chosen such that the midpoint of the fluid filament decreases exponentially with a constant stretching rate $\dot{\varepsilon}_0$ given by

$$\dot{\varepsilon}_0 = -\frac{2}{R_{mid}}\frac{d\,R_{mid}}{d\,t} \tag{1}$$

Selection of this velocity profile is complicated by the no-slip pinning condition imposed by the rigid endplates. Originally this selection was made ad hoc however recently several techniques for using open- or closed-loop feedback have been developed (Anna *et al.* 1999; Orr & Sridhar, 1999).

The fundamental benefit of a filament stretching rheometer is that the transient response of the same Lagrangian fluid element located at the column midplane is followed as a function of time, and that it experiences a constant stretching history. By contrast in other rheometric devices such as *Spinline Rheometers,* analysis of the kinematics and dynamical forces is complicated by the limited residence time of fluid elements in the spin-line and the nonhomogeneous stretching history they experience. The total Hencky strain experienced by the fluid elements at the midplane of a filament stretching device can be directly computed by integrating (1) to give

$$\varepsilon = \int_0^t \dot{\varepsilon}_0\, dt' = \ln\left[\left(R_0/R_{mid}(t)\right)^2\right] \tag{2}$$

Numerical simulations show that filament stretching devices can quantitatively measure the transient extensional stress growth function $\Delta\tau^+(\dot{\varepsilon}_0,t)$ of viscoelastic fluids (Sizaire & Legat, 1997; Kolte & Hassager, 1997; Yao & McKinley, 1998). Results are typically represented in dimensionless form in terms of the transient Trouton ratio $Tr = \Delta\tau^+/(\eta_0\dot{\varepsilon}_0)$ as a function of the Hencky strain and the Deborah number $De = \lambda_1\,\dot{\varepsilon}_0$. The stress relaxation following cessation of uniaxial elongation can also be measured (Spiegelberg & McKinley, 1997; Yao *et al.* 1998).

The characteristic forms of the tensile force response for a dilute polymer solution and an entangled viscoelastic material such as a concentrated polymer solution or polymer melt are shown in figure 2.

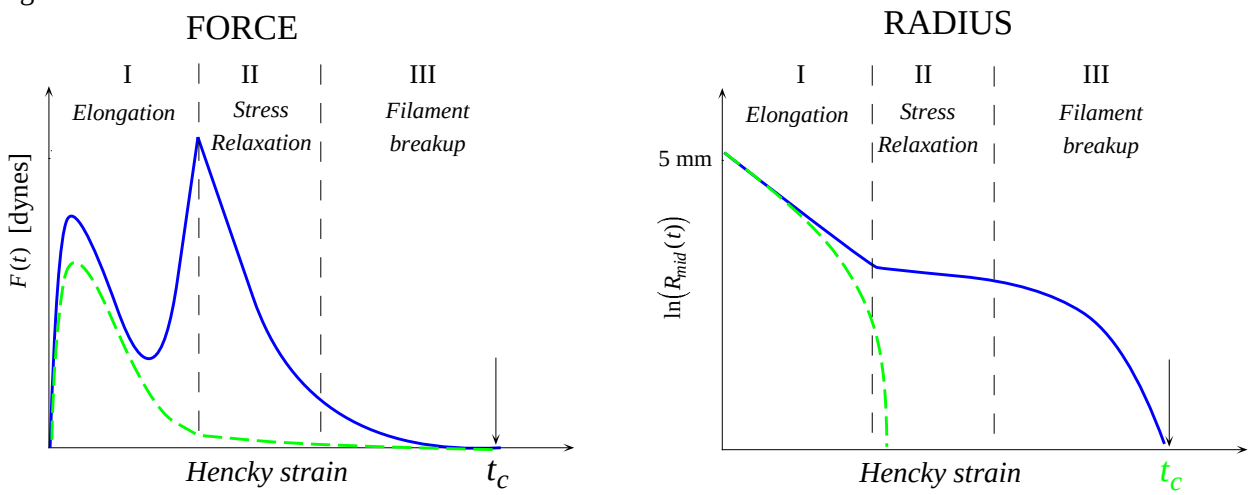

Figure 2. Characteristic form of the response in the force and midpoint radius for a dilute polymer solution (solid line) and a concentrated solution or melt (broken line).

During the imposed stretching, the force $F_z(t) = \Delta\tau^+(t) \times \pi R_{mid}(t)^2$ passes through a maximum at short times due to the exponential decrease in the area of the filament midplane and the (initially) small polymeric stresses. For a Newtonian fluid, the force continues to decrease monotonically; however for a strongly strain-hardening fluid it can increase again at later times. The approach to a steady-state uniaxial extensional viscosity in a polymeric filament is indicated by a second local maximum in the force at longer times. For a polymer melt, the initial growth in the force can be retarded due to the absence of a solvent (instantaneous) viscosity, and experiments show that the filament fails (i.e. breaks) shortly after force passes through a maximum. This failure of an elastic filament can be understand using a static stability construction taken from solid mechanics as we discuss in §4.3

3. Experimental results from Filament Stretching Devices

We first focus on experimental results obtained in model fluids such as dilute polymer solutions. The molecular/kinetic theory is best developed for such materials (Bird et al. 1987) and we can thus validate the performance of the device by comparing experimental results with theoretical predictions.

3.1 Dilute Polymer Solutions

Here we focus on a set of ideal elastic fluids consisting of a dilute concentration (0.05 wt%) of a monodisperse anionically-polymerized linear polystyrene chain dispersed in a low molecular weight oligomeric styrene. We study an homologous series of fluids denoted SM-1, SM-2, SM-3 containing 0.05 wt% of monodisperse polystyrene of molecular weights 2×10^6, 7×10^6 and 20×10^6 g/mol respectively. These fluids were prepared by Professor Susan Muller of UC-Berkeley as part of an ongoing round-robin study of the accuracy and reproducibility of the extensional stress growth measured by various filament stretching rheometers (Anna *et al.* 1999). The dynamic, steady and transient shear properties of these fluids have been thoroughly studied and coupled with intrinsic viscosity and light scattering measurements indicate that they are well-described by the Zimm Bead-Spring model incorporating hydrodynamic interactions. The dimensionless transient uniaxial stress growth measured in the filament stretching device for Fluid SM-1 is shown in Figure 3 for a range of Deborah numbers $8 \leq De \leq 60$. When plotted vs. the elapsed time of the experiment (scaled with the longest relaxation time λ_{Zimm}) the Trouton ratio is observed to grow increasingly rapidly at high *De*. However, if the results are plotted as a function of the total Hencky strain determined from eq. (2)), the material response is found to resemble a single master curve in which the extensional viscosity is solely a function of the applied strain. At low strains the stress is carried principally by the Newtonian solvent (the oligomeric styrene) and $Tr \approx 3\eta_s/\eta_0$. Beyond a strain of $\varepsilon \sim 2$, the stress climbs rapidly as the polymer chains elongate, and for strains $\varepsilon \geq 6$, the Trouton ratio approaches a steady state corresponding to full elongation of the polymer chains.

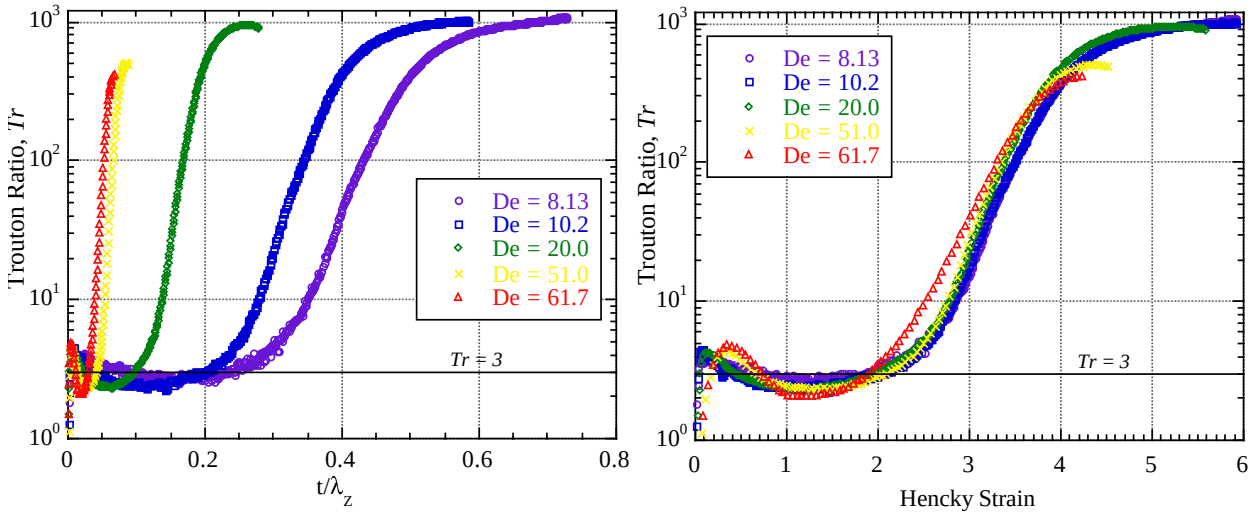

Figure 3. Transient Trouton ratio for fluid SM-1 (0.05 wt% monodisperse polystyrene in oligomeric styrene) for a range of Deborah numbers, $De \equiv \lambda_{Zimm}\,\dot{\varepsilon}_0$. The results are plotted (a) as a function of dimensionless time, t/λ_{Zimm} where λ_{Zimm} = 3.70 s. and (b) as a function of the total Hencky strain ε determined from equation (2).

3.2 Entangled polymer systems

In addition to measurement of the transient Trouton ratio for strongly strain-hardening dilute polymer solutions, it is also possible to use filament stretching devices to measure the transient stress growth in entangled systems such as concentrated polymer solutions and melts. Such fluids typically exhibit less pronounced stress growth; but accurate measurement of the extensional properties is nonetheless important in many polymer processing operations such as wet-spinning, roll-coating and container-filling. We have investigated the ability of the FISER to make extensional viscosity measurements in such materials using a concentrated solution (5 wt%) of high molecular weight polystyrene in a mixture of Tricresyl Phosphate and Dioctyl Phthalate (TCP/DOP). This system was chosen since extensive rheological characterization of the viscometric properties, together with measurements of the local stress differences in a complex flow have recently been published (Li *et al.* 1998). The fluid is strongly shear-thinning and well-described by a multi-mode version of the Giesekus constitutive model (Bird et al. 1987a). For such fluids, the need for comparison with numerical simulations is more pronounced since the stress growth is more moderate and the kinematics of the device are spatially nonhomogeneous. We have recently studied these effects in detail (Yao *et al.* 1998) and show below in Figure 4 the experimentally measured stress growth and the numerically predicted values obtained in a time-dependent simulation with a three-mode formulation of the Giesekus model. Excellent agreement between the experiments and simulations is observed; however, in order to obtain agreement with the predictions of ideal uniaxial elongation, it is essential that the force balance and kinematics of the fluid elements near the midplane are analyzed correctly. Further details of this analysis are provided in Kolte *et al.* 1997 and Yao *et al.* 1998.

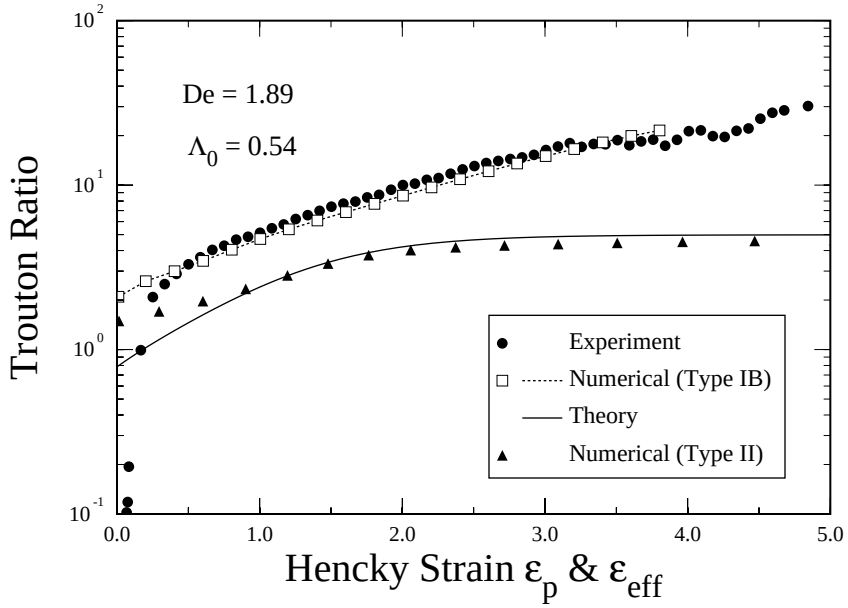

Figure 4. Transient Trouton ratio for a concentrated (5.0 wt%) polystyrene solution in DOP/TCP. Symbols show the experimentally measured stress growth, and the lines indicate the results of numerical simulation.

The FISER can also be used to measure the transient stress growth in polymer melts at room or elevated temperatures by encasing part or all of the translation stage in a tubular convection oven. This implementation is particularly useful for polymer melts of low to moderate viscosity such as nylon or PET since they are not rigid enough to support themselves in devices such as the Meissner rheometer (Meissner & Hostettler, 1994). Such an instrument is currently under construction in our laboratory and we plan to report further on these developments in the future.

4. Filament Failure

In addition to providing quantitative information about the stress growth during uniaxial elongation, devices such as FISER can be used to provide a means of investigating other poorly-understood viscoelastic phenomena that are frequently encountered during processing operations such as 'necking' and 'peeling'.

4.1 Cohesive Failure & Peeling

As the Deborah number $De = \lambda_1 \dot{\varepsilon}_0$ of the imposed stretching rate in the FISER is increased, the tensile viscoelastic stresses in the filament increase steadily. This may occur either because the stretching rate ($\dot{\varepsilon}_0$) of the deformation increases or because the longest relaxation time (λ_1) of the fluid increases. For the fluids SM–1, –2, –3 described in §3.1, the Zimm relaxation time scales as $\lambda_{Zimm} \sim M_w^{1.5}$ (Larson, 1988; Anna *et al.* 1999) and increases thirty-fold as the molecular weight increases from 2 to

20×10^6 g/mol. At such large stresses, elastic instabilities can arise during the stretching which lead to complete decohesion of the fluid column from the endplate. This instability originates from the large radial pressure-gradients that arise in the fluid near the rigid endplate as a result of the no-slip boundary condition (Spiegelberg *et al.* 1996).

As an example of the consequences of this *elastic end-plate instability*, we show in Figure 5 the dimensionless stress growth measured during elongation of the SM–1, –2 and –3 fluids at an identical extension rate of $\dot{\varepsilon}_0 = 2s^{-1}$, together with video-images of the radial profile of the elongating fluid column in the vicinity of the endplates.. The SM-1 fluid strain-hardens and smoothly approaches steady-state, by contrast, in the SM-2 and SM-3 fluids, the column elongates and becomes progressively more axially uniform until the bulk of the fluid is drained away from the endplate region. In order to elongate further, the fluid column then undergoes a symmetry-breaking instability of the free-surface near the rigid endplate. The rate of increase in the polymer stress is reduced and ultimately the entire filament *decoheres* from the endplate leaving a thin fluid film wetting the disk. The dynamics of this instability are closely related to those arising in peel tests of pressure sensitive adhesives (Ferguson *et al.* 1997; Piau *et al.* 1997) and filament stretching devices may be ideal for quantitative investigations of such phenomena.

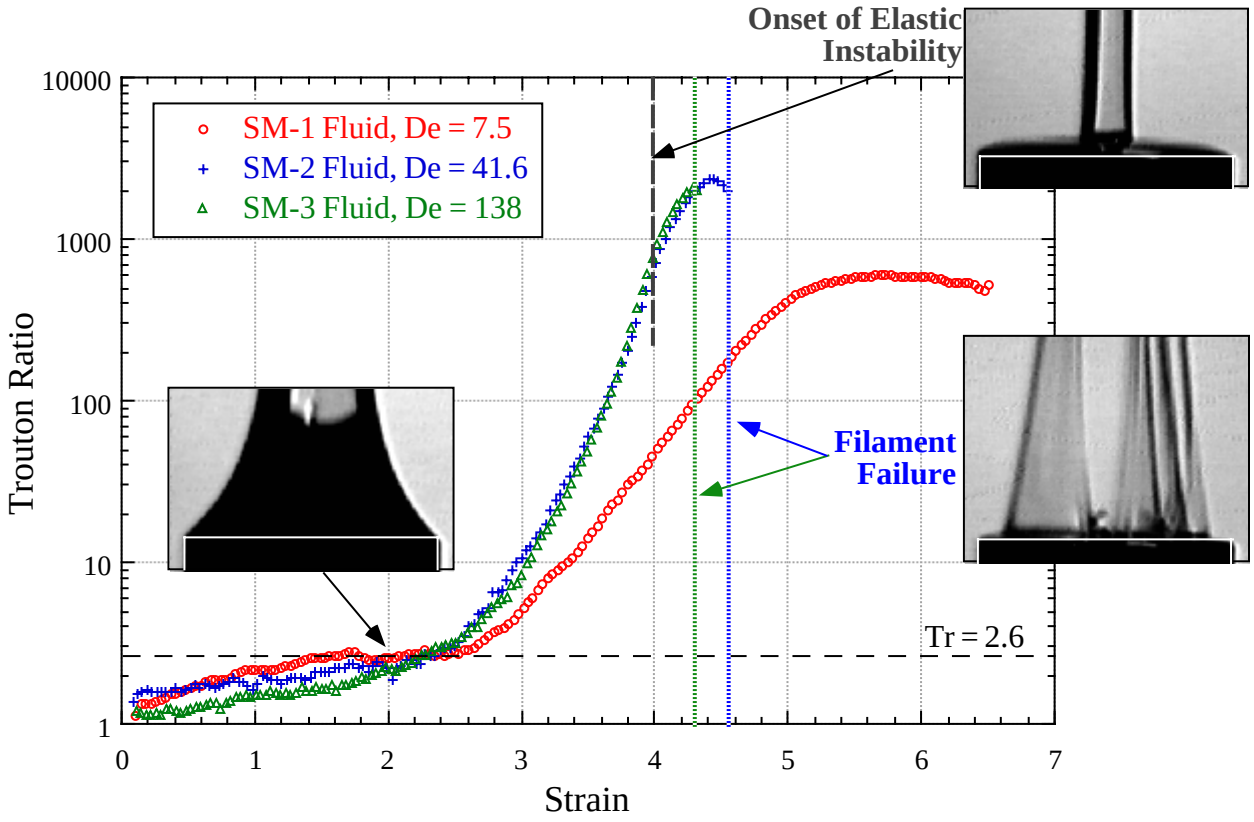

Figure 5 Elastic endplate instability and decohesion of strongly strain-hardening dilute polymer solutions SM-2 and SM-3.

In addition to quantifying the forces arising during this viscoelastic decohesion, the spatial dynamics of the instability can be readily imaged by constructing the lower disk of the filament stretching

rheometer out of glass or plexiglass and imaging the free surface from below. Plan-view images of the elastic endplate instability in a polyisobutylene/polybutene fluid are shown in figure 6 (Anna *et al.* 1997). The initial bifurcation is approximately azimuthally-periodic with a typical wavenumber of $m = 4$ or 5. As the instability proceeds, tip-splitting leads to a progressively finer structure. The initial periodic disturbances has recently been simulated in a fully-three-dimensional time-dependent free-surface viscoelastic flow simulation by Rasmussen & Hassager (1999).

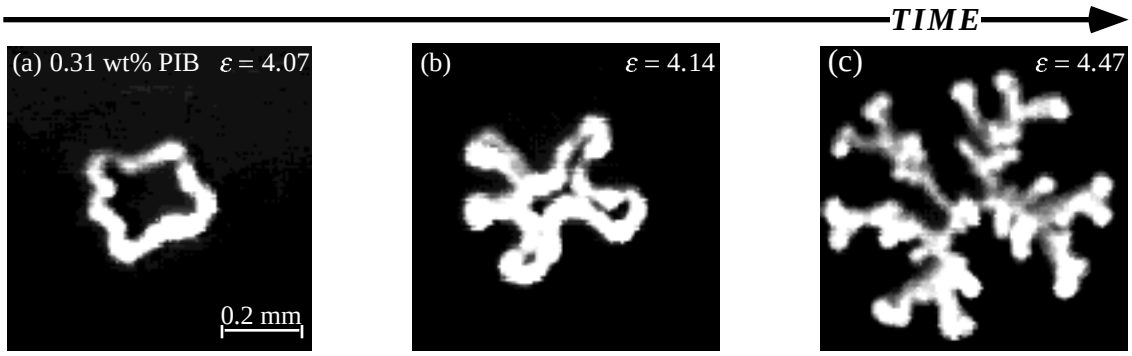

Figure 6. Plan view of the free surface perturbations during onset and growth of elastic end-plate instability in a PIB/PB polymer solution. The instability is cohesive in nature and a thin fluid film remains on the transparent plate through which the surface is imaged.

4.2 Elasto-capillary Thinning

Following the cessation of uniaxial elongation, the tensile stresses in the column rapidly and nonlinearly relax (Spiegelberg *et al.* 1996). As we have indicated in Figure 2, during this time the radius of the thin fluid column changes little for a strongly strain-hardening fluid such as a dilute polymer solution; by contrast for a less-strongly strain-hardening material such as an entangled solution or melt the radius may change very rapidly and the column breaks into two topologically distinct regions, each connected to an end-plate. The dynamics of this drainage and ultimate breakage can also be explored using the FISER.

Entov and co-workers (1990; 1997) have discussed the development of a *Microfilament Rheometer* and methods for analyzing the dynamics, and we follow their formulation. The slender fluid column with radial profile $R(z,t)$ slowly drains due to the capillary pressure $p_c \sim \sigma/R(z)$ (where σ is the surface tension coefficient) which is largest in the 'necked' region near the middle of the filament ($R \approx R_{mid}$). This necking is resisted by either a viscous stress (in the case of a Newtonian fluid) or by an elastic stress in a dilute polymer solution containing polymer chains that have previously been elongated by the imposed stretching phase. As a result, analysis (Entov & Hinch, 1997) shows that the midpoint radius of the filament evolves according to the following equations:

$$R_{mid}/R_0 = (\sigma/6\mu R_0)(t_c - t) \qquad \text{for a Newtonian fluid} \qquad (3)$$

and

$$R_{mid}\Big/R_0 = \left(GR_0/\sigma\right)^{1/3}\exp(-t/3\lambda_{Zimm}) \text{ for a bead-spring chain at intermediate times} \quad (4)$$

Here t_c is the critical time to breakup for a Newtonian fluid of viscosity μ whilst G is the elastic modulus of the viscoelastic fluid. For the bead-spring chain, at short times ($t \le \lambda_{Zimm}/\sqrt{2}$), the time-constants of multiple modes contribute to the stretching resistance. At long times, finite extensibility of the elongated polymer chains becomes important and the fluid filament fails like a Newtonian fluid of highly anisotropic viscosity with the radius decreasing linearly with time: however the relevant viscosity entering eq. (2) becomes the steady-state extensional viscosity $\bar{\eta}(\dot{\varepsilon}_0)$ which can be dramatically larger than the steady-shear viscosity η_0.

In Figure 7 we show a sequence of images summarizing the evolution of a Newtonian filament (oligomeric styrene) and a viscoelastic filament (fluid M-1). The characteristic formation of an axially-uniform cylindrical region connecting two fluid reservoirs can clearly be seen for the dilute polymer solution. As a consequence of the strain-hardening in the fluid, the filament life-time is increased from approximately 9 seconds to over 45 seconds. This stabilization of thin fluid filaments is directly connected to the *spinnability* of various fluids (Larson, 1983).

The midpoint radius $R_{mid}(t)/R_0$ is measured using a laser micrometer and the variation with time is shown in Figure 8(a). The Zimm relaxation time scales as $\lambda_{Zimm} \sim M_w^{1.5}$ and as the molecular eight is increased, the rate of elasto-capillary drainage decreases dramatically. The slope of the data in Figure 8(a) can be used to extract an independent measure of the dominant fluid relaxation during a string extensional flow, and it is clear from Figure 8(b) that for this class of dilute polymer solutions the data agrees extremely well with measurements from small-amplitude linear viscoelastic tests and with the predicted scaling from kinetic theory. Experiments on more complex materials such as adhesives with volatile solvents and telechelic polymer solutions (Winnik & Mheta, 1998) are currently underway and such measurements can be used to understand processing characteristics of these viscoelastic fluids in operations such as roll-coating which involve extensional flows and the creation of surface area followed by elasto-capillary drainage.

4.3 'Necking' Failure & the Considere criterion

For concentrated and entangled systems, numerical calculations show that the filament radius can neck down far more rapidly than observed in §4.2 (Yao *et al.* 1998) Such a response as indicated schematically in Figure 2. Indeed for sufficiently elastic materials, the filament may break even before the cessation of stretching (Kolte & Hassager 1997). This process can be understood in terms of the Considère criterion that characterizes the necking failure of solid polymer samples undergoing uniaxial extension (Coggswell, 1972; Malkin & Petrie, 1996). This static energy stability criterion is derived from the principle of virtual work and states that if the tensile force in the elastic

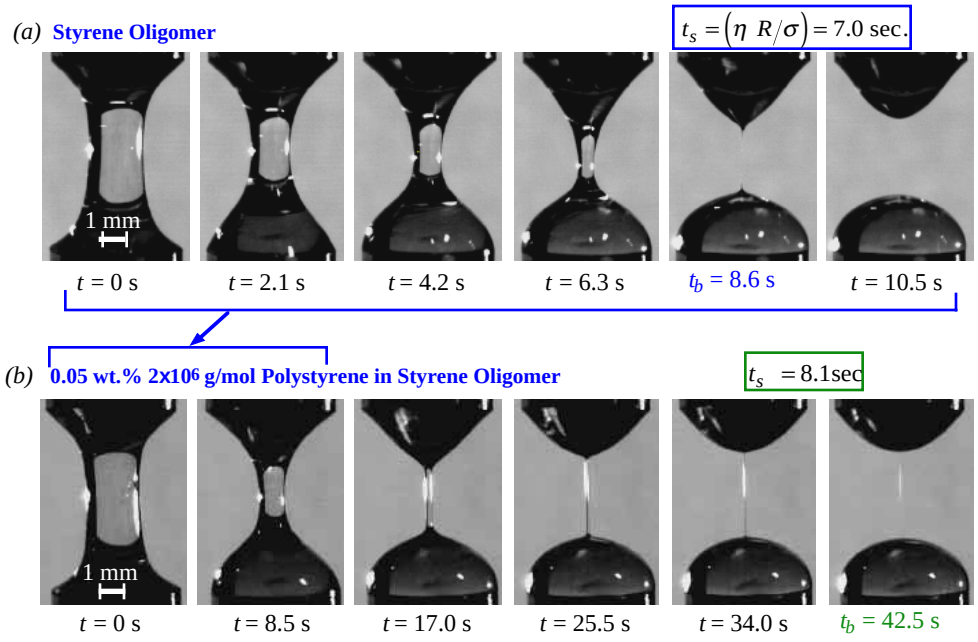

Figure 7 Video images of the filament breakup of *(a)* a Newtonian fluid (viscous styrene oligomer) and *(b)* a dilute polymer solution containing 500ppm of monodisperse polystyrene (SM-1). The addition of viscoelasticity changes the dominant balance of forces in the thinning filament from *visco-capillary* thinning in *(a)* to *elasto-capillary* thinning in *(b)*. The spatial evolution in the filament profile is changed and the time to breakup t_b is increased from 8.6 s to 42.5 s.

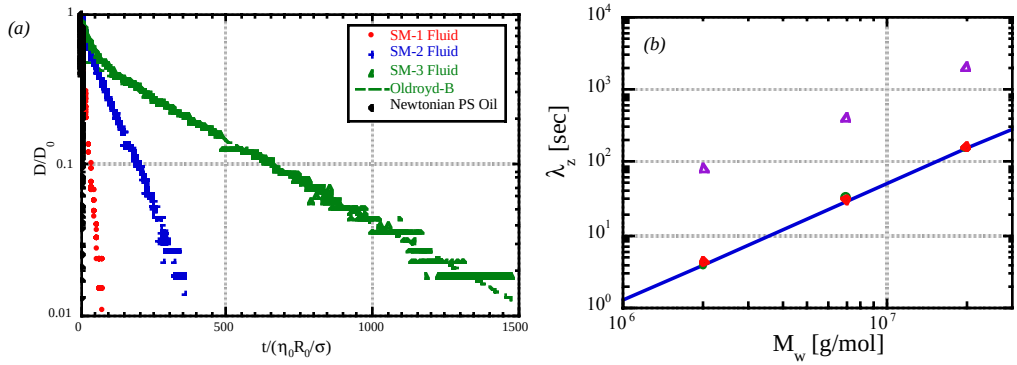

Figure 8 Variation in the rate of of necking and time to breakup (t_b) of the viscous Newtonian oil and 3 dilute monodisperse polystyrene solutions as the molecular weight is varied; SM-1 = 2×10^6 g/mol, SM-2 = 7×10^6 g/mol, SM-3 = 20×10^6 g/mol. *(a)* The measured midpoint diameter $D(t) = 2R(t)$ as a function of dimensionless time, t/t_s; *(b)* Scaling of the longest (Zimm) relaxation time obtained from steady shear (○), from filament breakup (◆), and the critical time to breakup (△) with mol. wt.

filament passes through a maximum then infinitesimal perturbations will grow spontaneously and a neck will propagate. Since the dimensionless force is $f(t) \equiv F_z / \left(\pi R_0^2\ \eta_0 \dot{\varepsilon}_0\right)$ this condition can be rearranged in terms of the Trouton ratio to give the following stability condition (valid for large *De* when elastic effects are dominant)

$$\frac{d \ln Tr}{d\varepsilon} > 0 \qquad \text{for stable extension} \qquad (5)$$

i.e. it is not sufficient for the Trouton ratio to simply increase, it must increase at least exponentially fast with the strain. For materials with a bounded extensional viscosity, this stability criterion is violated at a critical strain ε_{crit}, and the material will fail, regardless of how careful the sample preparation has been. We have recently analyzed the implications of this stability criterion for the Doi-Edwards model for entangled linear homopolymers and for the 'Pom-Pom' model of McLeish & Larson (1998) that describes a series of prototypical branched molecules (McKinley & Hassager, 1999). In the *rapid stretching limit* corresponding to $De >> 1$ analytical answers can be obtained in a number of model stretcing flows such as transient uniaxial, biaxial and planar elongation. As an example, we find that in transient uniaxial elongation the critical strain to failure for the 'Pom-Pom' model is

$$\varepsilon_{crit} = \ln\left(q\sqrt{3}\right) \tag{6}$$

where q is the number of branched arms off the chain backbone. This result provides a rational explanation for the well-known stabilization of film-blowing and fiber-drawing processes that arises from the addition of small quantities of branched polymer such as LDPE. The Considère criterion can be represented on a plot of the transient Trouton ratio predicted for the 'Pom-Pom' model as shown below in Figure 9.

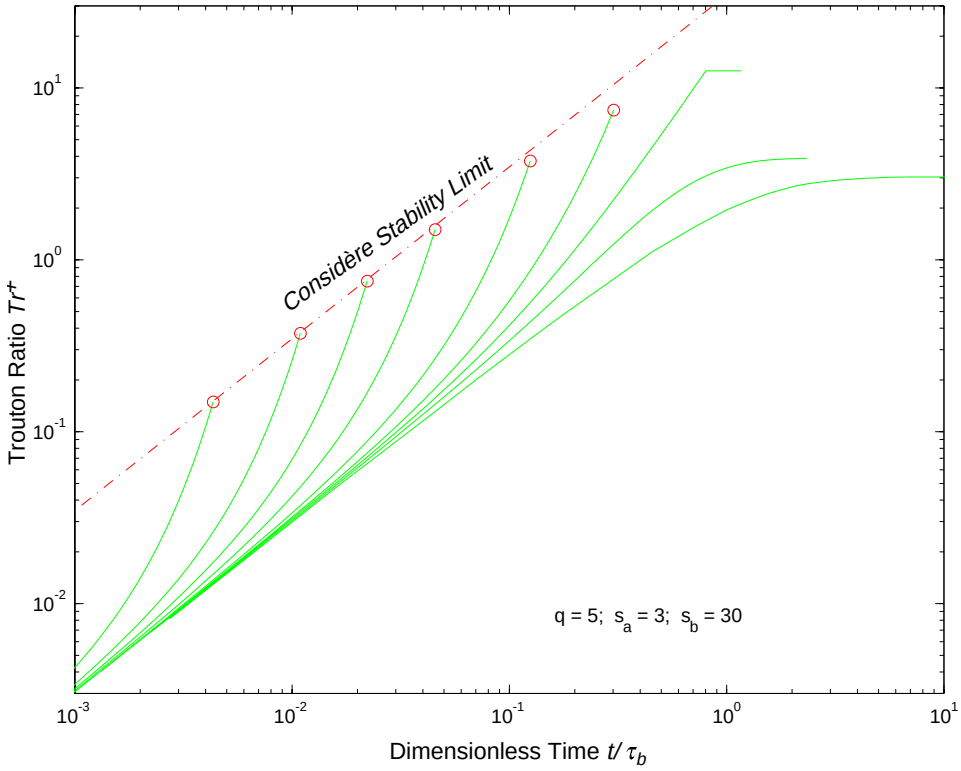

Figure 9. Consequences of the Considère stability criterion on the transient stress growth as measured in a melt tensiometer or filament stretching device, for a branched material with q = 5 arms off the main chain backbone. The arms have, on average, $s_a = 3$ entanglements and the backbone has $s_b = 5$ entanglements.

The necking instability prevents the extensional viscosity from being measured beyond a critical strain. For the 'pom-pom' model, in the rapid-stretching limit, the corresponding maximum value of the Trouton ratio lies a fixed factor of $\left(q^2/\ln(\sqrt{3}\,q)\right)$ above the linear viscoelastic envelope as shown in Figure (9). This upper bound corresponds closely to the truncation in the transient stress growth data frequently observed in branched polyethylene melts (cf. For example Meissner, 1985; Munstedt *et al.* 1998; Inkson *et al.* 1999). This suggests a method for rapidly estimating the characteristic level of branching (q) in a particular polymeric material.

5 Conclusions

In this paper we have examined some recent developments in extensional rheometry of viscoelastic liquids such as polymer melts and solutions. The Filament Stretching Rheometer (FISER) provides a means of probing the stress growth during transient uniaxial elongation; whereas the microfilament rheometer (MFR) developed by Entov & co-workers permits analysis of the subsequent relaxation processes during cessation of stretching. In addition to enhancing our understanding of the rheology of the test materials, analysis of the instabilities that arise in these devices such as the elastic endplate instability and the rapid necking of the filaments can also be used to shed new light on poorly-understood phenomena such as the 'tackiness' and 'spinnability' of various polymeric fluids.

Acknowledgements

This research has been supported by the National Science Foundation, Chemical & Thermal Systems Division and the NASA Microgravity Fluid Dynamics Program. Additional support from the Lord Foundation of Massachusetts is gratefully acknowledged. GHM would like to thank Prof. O. Hassager for numerous detailed discussions of many of the issues presented in this paper.

References

Anna, S.L., McKinley, G.H., Sridhar, T.S., James, D.F. and Muller, S.J., filament Stretching Rheometry for Dilute Polymer Solutions: A Round-Robin Study, *J. Rheol.*, (1999), in preparation.

Anna, S.L., Spiegelberg, S.H. and McKinley, G.H., Elastic Instability in Elongating Filaments, *Phys. Fluids*, **9**(9), (1997), S10 (Gallery of Fluid Motion).

Bazilevsky, A.V., Entov, V.M. and Rozhkov, A.N., "Liquid Filament Microrheometer and Some of its Applications", Third European Rheology Conference, D. R. Oliver (ed.), Elsevier Applied Science, 1990.

Bird, R.B., Armstrong, R.C. and Hassager, O., Dynamics of Polymeric Liquids. Volume 1: Fluid Mechanics, Vol. 1, 2nd Edition, Wiley Interscience, New York, 1987.

Bird, R.B., Curtiss, C.F., Armstrong, R.C. and Hassager, O., Dynamics of Polymeric Liquids. Volume 2: Kinetic Theory, Vol. 2, 2nd Edition, Wiley Interscience, New York, 1987.

Cogswell, F.N. and Moore, D.R., A Comparison Between Simple Shear, Elongation and Equal Biaxial Extension Deformations, *Polym. Eng. and Science*, **14**(8), (1974), 573-576.

Entov, V.M. and Hinch, E.J., Effect of a Spectrum of Relaxation Times on the Capillary Thinning of a Filament of Elastic Liquid, *J. Non-Newt. Fluid Mech.*, **72**(1), (1997), 31-54.

Ferguson, J., Reilly, B. and Granville, N., Extensional and Adhesion Characteristics of a Pressure Sensitive Adhesive, *Polymer*, **38**(4), (1997), 795-800.

Hassager, O., Kolte, M.I. and Renardy, M., Failure and Nonfailure of Fluid Filaments in Extension, *J. Non-Newt. Fluid Mech.*, **76**(1-3), (1998), 137-152.

Inkson, N.J., McLeish, T.C.B., Harlen, O.G. and Groves, D.J., Predicting Low Density Polyethylene Melt Rheology in Elongational and Shear Flows with "Pom-Pom" Constitutive Equations, *J. Rheol.*, (1999), submitted.

James, D.F. and Walters, K.A., "A Critical Appraisal of Available Methods for the Measurement of Extensional Properties of Mobile Systems", Techniques in Rheological Measurement, A. A. Collyer (ed.), Elsevier, London, 1993.

Kolte, M.I., Rasmussen, H.K. and Hassager, O., Transient Filament Stretching Rheometer II: Numerical Simulation, *Rheol. Acta*, **36**, (1997), 285-302.

Larson, R.G., Spinnability and Viscoelasticity, *J. Non-Newt. Fluid Mech.*, **12**, (1983), 303-315.

Larson, R.G., Constitutive Equations for Polymer Melts and Solutions, Series in Chemical Engineering, Butterworths, Boston, 1988.

Li, J.-M., Burghardt, W.R., Yang, B. and Khomami, B., Flow Birefringence and Computational Studies of a Shear-Thinning Polymer
Solution in Axisymmetric Stagnation Flows, *J. Non-Newt. Fluid Mech.*, **74**(1-3), (1998), 151-194.

Malkin, A.Y. and Petrie, C.J.S., Some Conditions for Rupture of Polymeric Liquids in Extension, *J. Rheol.*, **41**(1), (1997), 1-25.

McKinley, G.H. and Hassager, O., The Considère condition and Rapid Stretching of Linear and Branched Polymer Melts, *J. Rheol.*, (1999), submitted.

Meissner, J., Experimental Aspects in Polymer Melt Elongational Rheology, *Chem. Eng. Commun.*, **33**, (1985), 159-180.

Meissner, J. and Hostettler, J., A New Elongational Rheometer for Polymer Melts and Other Highly Viscoelastic Liquids, *Rheol. Acta*, **33**(1), (1994), 1-21.

Münstedt, H., Kurzbeck, S. and Egersdörfer, L., influence of Molecular Structure on Rheological Properties of Polyethylenes, *Rheol. Acta*, **37**, (1998), 21-29.

Orr, N.V. and Sridhar, T.S., Probing the Dynamics of Polymer Solutions in Extensional Flow Using Step Strain-Rate Experiments , *J. Non-Newt. Fluid Mech.*, **80**, (1999)

Piau, J.-M., Verdier, C. and Benyahia, L., Influence of Rheology and Surface Properties in the Adhesion of Uncross-linked Pressure Sensitive Adhesives, *Rheol. Acta*, **36**, (1997), 449-461.

Rasmussen, H.K. and Hassager, O., Three-Dimensional Simulations of Viscoelastic Instability in Polymeric Filaments, *J. Non-Newt. Fluid Mech.*, **82**(2-3), (1998), 189-202.

Sizaire, R. and Legat, V., Finite Element Simulation of a Filament Stretching Extensional Rheometer, *J. Non-Newt. Fluid Mech.*, **71**(1-2), (1997), 89-108.

Spiegelberg, S.H., Ables, D.C. and McKinley, G.H., The Role of End-Effects on Measurements of Extensional Viscosity in Viscoelastic Polymer Solutions With a Filament Stretching Rheometer, *J. Non-Newtonian Fluid Mech.*, **64**(2-3), (1996), 229-267.

Spiegelberg, S.H. and McKinley, G.H., Stress Relaxation and Elastic Decohesion of Viscoelastic Polymer Solutions in Extensional Flow, *J. Non-Newtonian Fluid Mech.*, **67**, (1996), 49-76.

Tirtaatmadja, V. and Sridhar, T., A Filament Stretching Device for Measurement of Extensional Viscosity, *J. Rheol.*, **37**(6), (1993), 1081-1102.

van Nieuwkoop, J. and Muller von Czernicki, M.M.O., Elongation and Subsequent Relaxation Measurements on Dilute Polyisobutylene Solutions, *J.Non-Newt. Fluid Mech.*, **67**, (1996), 105-124.

Winnik, M.A. and Yekta, A., Associative Polymers in Aqueous Solution, *Curr. Opin. Coll. & Int. Sci.*, **2**, (1997), 424-436.

Yao, M. and McKinley, G.H., Numerical Simulation of Extensional Deformations of Viscoelastic Liquid Bridges in Filament Stretching Devices, *J. Non-Newtonian Fluid Mech.*, **74**((1-3)), (1998), 47-88.

Yao, M., McKinley, G.H. and Debbaut, B., Extensional Deformation, Stress Relaxation and Necking Failure of Viscoelastic Filaments, *J. Non-Newtonian Fluid Mech.*, **79**(Special Issue dedicated to 60th birthday of M. Crochet), (1998), 469-501.